

Beam Selection Algorithm Based On PTR Metric and its Synchronization Performance

by

Lu Dong and Mary Ann Ingram

{ludong, mai}@ece.gatech.edu

School of Electrical and Computer Engineering
Georgia Institute of Technology

Copyright © 2003 IEEE. Reprinted from the IEEE Radio and Wireless Conference, Aug. 2003. This material is posted here with permission of the IEEE. Internal or personal use of this material is permitted. However, permission to reprint/republish this material for advertising or promotional purposes or for creating new collective works for resale or redistribution must be obtained from the IEEE by sending a blank email message to pubs-permissions@ieee.org. By choosing to view this document, you agree to all provisions of the copyright laws protecting it.

Beam Selection Algorithm Based on PTR Metric and Its Synchronization Performance

Lu Dong, Mary Ann Ingram, *Member, IEEE*
School of Electrical and Computer Engineering
Georgia Institute of Technology Atlanta, Georgia 30332-0250
Email: ludong@ece.gatech.edu; mai@ece.gatech.edu

Abstract—A switched-beam beamformer is combined with a multi-receiver architecture to improve the signal-to-interference-and-noise-ratio (SINR) for indoor wireless LANs. The multiple selected beams can be used for diversity combining and for multiple-input multiple-output (MIMO) links. The beam selection controller uses two metrics, the received signal strength indication (RSSI) and the peak-to-trough ratio (PTR), to iteratively select beams with good SINR. The second metric prevents beam falsing. This paper will describe the receiver system and the associated beam selection algorithm, and presents the relationship between the PTR and SINR. The paper also shows that the beam selection algorithm based on the PTR is robust to synchronization offsets for 802.11a and 802.16 waveforms.

I. INTRODUCTION

The array antenna with switched beamforming has been recognized as a good method to combat multipath fading of the desired signal and to suppress interference [1], [2]. Compared with fully adaptive antennas, switched-beam antennas do not have the high computation and implementation complexity, but still can gain high SIR improvement in interference-limited environment [3]. The multiple selected beams can be used for diversity combining and for multiple-input multiple-output (MIMO) links. However, beam-falsing, which is the most serious loss in switched-beam antennas, occurs because the selected beams may not be the best beams. One common method for beam selection is choosing beams with the largest received powers based on the (RSSI). But it is possible that the wrong beams are chosen since RSSI does not distinguish between desired signal and interference.

In [3], a dual-metric beam selection algorithm is proposed. The first metric, RSSI, is intended to be measured by an analog detector, while the second metric, BER, could be measured, in theory, in the digital signal processor (DSP). The goal in [3], as it is here, is to make a selection

The authors wish to thank the Yamacraw Mission, of the state of Georgia, U.S.A. <http://www.yamacraw.org> for partially supporting this research.

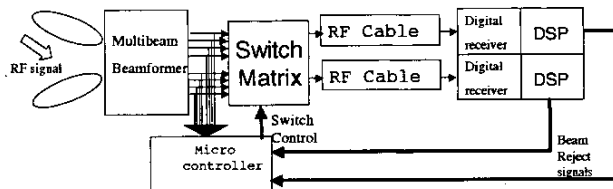


Fig. 1. System schematic

using only two full radio chains. However, BER is not a practical metric because it requires a time-consuming calculation. It is the goal of this paper to present a practical “second” metric, which we call the peak-to-trough (PTR) metric.

The PTR metric is related to the metric of [4], which is a beam selection method based on signal validation. The PTR relies on a sequence of unique words periodically embedded in the transmitted symbol sequence. Beams with the highest cross-correlation with unique words are selected.

II. SYSTEM STRUCTURE

We apply this beam selection algorithm into the 2 × 2 MIMO system. The transmitter consists of two omnidirectional antennas. The switched-beam receiver system uses two selected beams. Two possible configurations for the receive antennas are as follows: (1) Two antenna arrays, each followed by a multibeam beamformer [5]; one beam is selected from each beamformer to form the two selected beams; (2) one antenna array followed by one multibeam beamformer. An associated switch matrix will choose 2 of the beams. In configuration (2), one selected beam nearly always yields a lower average power than the other selected beam, leading to diminished diversity performance [6]. Therefore, configuration (1) has the advantage that the two selected beams could both point in the same direction, and yield comparable average powers and uncorrelated fading.

The system schematic is shown in Fig. 1. The microcontroller first arranges the beams based on RSSI. The sensors, which test each beam's strength, are on the switch matrix board. They send the measured RSSI to the controller immediately. The beams with the two highest RSSI are selected. Then the second metric tests whether there is too much interference in the beams. If there is not much interference, the two selected beams will not change. Otherwise, one or two beam rejection signals are sent from the DSP to cause the rejected beam (or beams) to be replaced by the next strongest beam (or beams).

This "second" metric, the PTR metric, is discussed in next section.

III. PTR METRIC PRINCIPLE AND EXPERIMENT RESULT

In the orthogonal frequency division multiplexing (OFDM) standards 802.11a [7] and 802.16 [8], training symbols are embedded into physical layer preambles as the unique words. Figs. 2 and 3 show the training structures in the 802.11a and 802.16 standards, which have ten and five short training symbols, respectively.

According to [3], we first arrange the beams in order of descending RSSI. Then, we check the beams' PTR values in order. If the PTR value is less than a threshold (which can be set based on real system's requirement), we conclude that this beam has too much interference and noise; then we check the next strongest beam until we find a PTR value that is higher than the threshold.

To get the PTR metric, we use the following equation

$$R_x(m) = \frac{\left| \sum_{n=0}^{N1} \bar{r}_x(n+m) \bar{t}_x^*(n) \right|}{\left| \sum_{n=0}^{N1} \bar{r}_x(n+m) \bar{r}_x^*(n+m) \right|}, \quad (1)$$

$$m = 0, 1, 2, \dots, N2$$

where r_x is the received short training sequence which includes noise and interference, and t_x is the original one-period-long training sequence. $N1$ is the length of one period of the training sequence (16 symbols for 802.11a and 64 symbols for 802.16). $N2$ is the length of the whole short training sequence plus one period length (for 802.11a, it is $10 \cdot N1 + N1 = 176$, for 802.16, it's $5 \cdot N1 + N1 = 384$). $R_x(m)$ is the normalized cross-correlation function. If the received signal includes limited noise and interference, $R_x(m)$ will have $N2/N1-1$ peaks. Then each peak and some points on each side of it are removed. The remainder depends on the correlation of the training sequence with the noise and interference.

The second metric is computed as

$$PTR = \frac{\langle (\text{magnitude of the peaks})^2 \rangle}{\langle (\text{magnitude of the remainder})^2 \rangle} \quad (2)$$

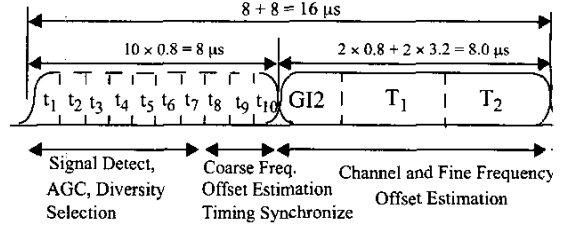


Fig. 2. 802.11a OFDM training structure

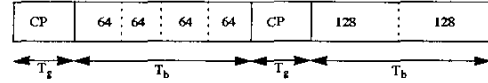


Fig. 3. 802.16 OFDM training structure

Where $\langle \rangle$ indicates a time average.

Figs. 4 and 5 show the results of an wired hardware test of the PTR metric. The 802.11a preamble was generated at IF and we set the length of one period of training sequence 64 instead of 16. The IF signal was added to the output of a noise generator using a power combiner and then sampled, downconverted. The PTR metric was computed in the digital receiver's DSP. Fig. 4 is the result of the sliding correlation of the 802.11a preamble with one OFDM training symbol with the noise generator off. The peaks and troughs of the correlation are clear. Next, varying amounts of noise were added, and the PTR was computed for 10 trials for each noise value. The sample values of the PTR metric for each noise power value are shown in Fig. 5. An example beam reject threshold is shown. The figure shows that the PTR is an effective indicator of SNR.

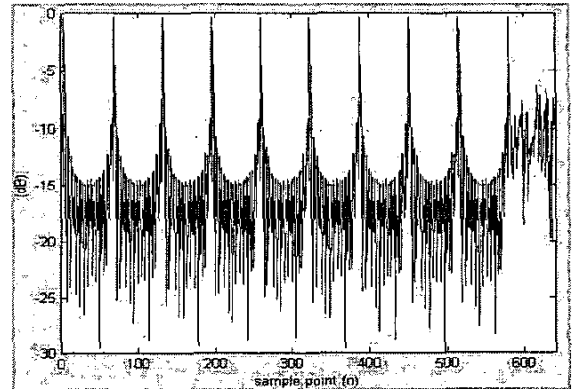


Fig. 4. The cross-correlation output

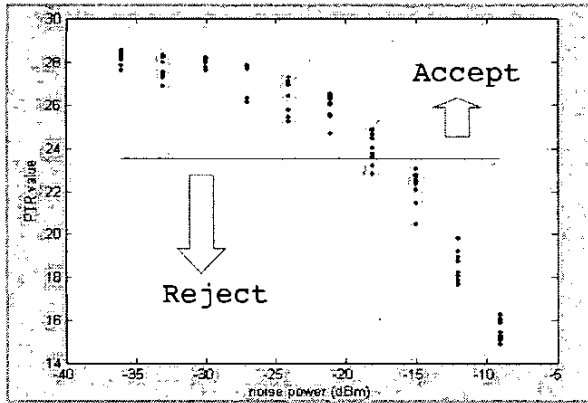


Fig. 5. PTR with different noise powers

IV. PTR METRIC'S SYNCHRONIZATION PERFORMANCE

Because this PTR beam-selection algorithm operates directly on the IF signal, it has fast feedback ability and doesn't need more digital signal processing such as diversity combining. We also hope no synchronization will be performed before the PTR calculation. Otherwise the feedback will be delayed and degrade the accuracy for beam selection in a time varying channel like indoor wireless environment.

Therefore, we should test whether the PTR metric is robust enough to the synchronization offsets: frequency offset, sampling frequency offset and frame time offset. Another type of offset, carrier phase offset, obviously has no impact on PTR metric from equations (1) and (2).

For the 802.11a standard, the transmit center frequency tolerance is 20 parts per million (ppm) maximum, ($5GHz \cdot 20ppm = 100kHz$). The symbol clock frequency tolerance is 20 ppm maximum. About frame time offset, based on the algorithm of searching the beginning of short training sequence, error within 0.1 period is guaranteed. That is $0.8 \cdot 0.1 = 0.08\mu s$.

PTR versus SINR curves for different types of synchronization offsets are shown in Figs. 6, 7 and 8. We assume that the interference is uncorrelated with the short training symbols. We observe that the PTR monotonically increases with SINR, with a nearly linear characteristic in the 0 to 15 dB range. Even when the synchronization offset is higher than the tolerance value in the standard, the curves are not changed much. In the frame time offset picture, we choose a very big value ($1.5\mu s \gg 0.08\mu s$). So we can see an obvious change of the curve when the SINR is above 10 dB. But this case will absolutely not happen. The little change of the curves with the synchronization offset values indicates the robustness of PTR metric under offset conditions.

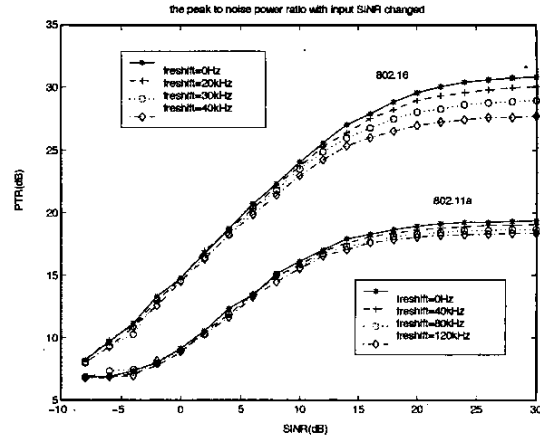


Fig. 6. PTR under Frequency offset

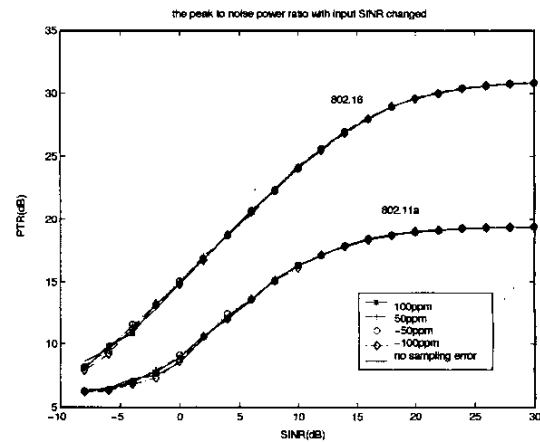


Fig. 7. PTR under sampling offset

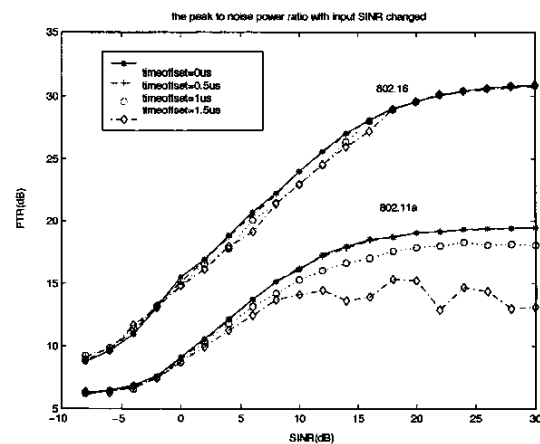


Fig. 8. PTR under frame time offset

We can get very similar synchronization performance results for the two standards. For 802.16, we should notice that the carrier frequency is 2.4GHz, and the frequency accuracy tolerance is ± 15 ppm maximum. So the frequency offset will be limited under $2.4GHz \cdot 15ppm = 36kHz$. This time, in the frame time offset situation, even when we choose the very big value ($1.5\mu s$), the curves are still not changed much. Because of the relatively low carrier 2.4GHz, the PTR metric becomes more robust against the time offset.

V. CONCLUSION

This paper describes our mutibeam receive system and the principle of the PTR metric beam-selection algorithm. Combined with RSSI selection, the PTR metric will select beams that have both good desired signal gain and little probability to include large noise and interference.

Through analysis and simulation, we found PTR metric is very robust to synchronization offsets for 802.11a and 802.16 waveforms.

REFERENCES

- [1] J.H. Winters, "Smart Antennas for Wireless Systems," *IEEE Personal Communications*, vol. 5, no. 1, pp. 477-482, Feb. 1998.
- [2] T. Moorti and A. Paulraj, "Performance of switched beam systems in battlefield TDMA networks," *Military Communications Conference, Conference Proceedings, IEEE*, vol. 1, no. 21-24, pp. 215-219, Oct. 1996.
- [3] K.-H. Li and M. A. Ingram, "Space-time block-coded OFDM systems with RF beamformers for high-speed indoor wireless communications," *IEEE Transactions on Communications*, vol. 50, no. 12, pp. 1899-1901, Dec. 2002.
- [4] T. Matsumoto, S. Nishioka, and D.J. Hodder, "Beam-selection performance analysis of a switched multibeam antenna system in mobile communications environments," *IEEE Transactions on Vehicular Technology*, vol. 46, no. 1, pp. 10-20, Feb. 1997.
- [5] Bruno Pattan, *Robust Modulation Methods and Smart Antennas in Wireless Communication*, Prentice Hall PTR, 2000.
- [6] Kuo-hui Li, *RF beamformers for High-speed Wireless Communication*, Ph.D Thesis, Georgia Institute of Technology, 2000.
- [7] IEEE 802.11a, *Part 11: wireless LAN Medium Access Control (MAC) and Physical Layer PHY specifications*, LAN/MAN Standards Committee, 1999.
- [8] IEEE 802.16a/D4 2002, *Part 8: Physical Layer*, LAN/MAN Standards Committee, 2002.